



Comparative Investigation of the Energy Efficiency of Mini-Split Air Conditioning with Variable Refrigerant Flow Systems for Office Buildings in Hot Climate

Received 17 October 2023; Revised 1 February 2024; Accepted 1 February 2024

Ahmed A. Hussien ¹
Ahmed Hamza H. Ali ²
Ibrahim M. Ismail ³

Keywords

Variable Refrigerant Flow;
Mini-split air-conditioning;
energy-saving, HVAC.

Abstract: The use of air conditioning systems is a major contributing factor to Egypt's growing electricity consumption, which is a serious problem, particularly in arid and hot regions like Aswan City. This study compares the energy-saving capabilities of two air conditioning systems for office buildings in Aswan City: a variable refrigerant flow system (VRF) and a mini-split air conditioning (MSAC) unit. TRNSYS software is used in the analysis. Examining their energy efficiency and applicability to power usage concerns is the primary objective. The principal findings are unambiguous. Particularly in the summer when it's hot outdoors, the VRF system consistently demonstrates a discernible benefit in terms of energy efficiency. By converting to the VRF system, a substantial yearly energy savings of roughly 19,187.43 kWh can be realized. The projected energy efficiency ratio between the MSAC system and the VRF system is 0.746. The VRF system conserves more energy than the MSAC system by 25.4%, which demonstrates how energy-efficient it is. With 8.29-year payback times, the VRF system performed better than the MSAC system. Furthermore, during the period of the cooling system's life, the VRF system greatly reduced CO₂ emissions; when fuelled by coal, oil, or natural gas, respectively, this reduction came to 26.03% (14.58, 11.59, and 8.23 metric tonnes) less than the MSAC system. These outcomes highlight the environmental advantages of the VRF system and its potential as an energy-efficient and ecologically friendly cooling solution.

1. Introduction

At the 21st session of the Conference of the Parties (COP21) on climate change in Paris, France, in December 2015, world leaders signed an agreement for the first time in climate

¹ Department of Mechanical Engineering, Assiut University, Assiut, Egypt

² Department of Mechanical Engineering, Assiut University, Assiut, Egypt

³ Department of Mechanical Engineering, Assiut University, Assiut, Egypt

negotiation history. The goal of the Paris Agreement is to pursue measures to keep the rise in the average worldwide temperature to 1.5 °C above the level of pre-industrial times and to keep it well below 2 °C above that of pre-industrial times. Since energy production and consumption account for the two primary sources of worldwide greenhouse gas emissions, the energy sector is essential to reaching this goal [1]. In addition, inefficiency has been a prevalent aspect of energy use in most Middle East and North African countries for the past few decades; high retail energy price subsidies covered this fact for years, but as oil prices declined, this was no longer possible due to reduced revenues. However, global warming is a major threat to all countries worldwide, particularly to the Middle East and North Africa region [2]. Over the past 20 years, Egypt's average temperature has increased significantly, which has increased the country's energy requirement for summer cooling. According to climate estimates, Egypt is expected to suffer higher warming than the global average by 2100. Additionally, the country would confront a notable rise in electricity demand due to the increased frequency of extreme heat events, urbanisation, and population expansion. Temperature increases might put natural gas, solar PV, and wind power generation under more strain, lowering efficiency. A more resilient energy system is required due to the rising demand for cooling power and the declining efficiency of generation [3].

Residential and commercial structures account for nearly half of Egypt's total electricity use. It is anticipated that this percentage will rise as a result of global warming [4]. Building consumption is predicted to rise, as it has over the past ten years—from 150 GWh in 2009 to 217 GWh in 2017—due to population growth, which has led to an increase in the number of buildings. Additionally, as external temperatures rise as a result of the global warming effect, building consumption is expected to rise while occupant thermal comfort levels remain the same [2], [5]. Arafat et al. carried out research that aims to enhance the sustainability of university buildings by implementing a unique weighting system based on Egypt's Green Pyramid Rating System. A questionnaire was developed with stakeholder input and assessed using statistical methodologies and the analytical hierarchy process. The results show that Energy Efficiency (EE) has the highest weight (21%), followed by water efficiency (19%), Indoor Environmental Quality (IEQ) and sustainable Sites (17%), materials and resources (14%), and management protocols (12%)[6]. Fahmy et al. explored the development of new Egyptian cities with distinct urban identities and architectural features, focusing on climate-responsive neighbourhood planning and eco-friendly materials. It uses the Urban-Building-Materials-Renewables (UBMR) methodology to promote sustainable urban design strategies in arid regions. Comparative analysis of parcel division planning and courtyarded clustered free planning in Cairo shows improved outdoor comfort, increased solar energy generation, reduced cooling energy consumption, and substantial construction cost reduction. Combined UBMR solutions improved outdoor comfort by 47.8% during intense hot afternoons, boosted yearly solar energy generation potential by 13.87%, and the energy-efficient envelope lowered cooling energy usage by 28.9% while lowering construction costs by 95.5% [7]. Galal et al. focused on outdoor thermal comfort while examining the viability of densification in the new cities of Upper Egypt. It makes use of information from microclimate models, climatic observations, and

site surveys. The findings indicate that, depending on location and street direction, densification lowers average Physiological Equivalent Temperature (PET) values by 1 °C over the course of the quarter and by up to 5.5 °C in some of the evolved regions throughout the day. The results point to possible adjustments to planning guidelines or policies for the expansion of settlements in arid climates[8]. HVAC systems, also known as heating, ventilation, and air conditioning, include air conditioning systems. Modern design and selection consider architecture, energy consumption, installation, indoor air quality, thermal comfort, and economics, and cost implications. Designers aim to create the most effective HVAC systems for various applications.

An urgent problem in Egypt is the high electricity consumption levels brought on by the widespread use of air conditioning equipment in buildings. Particularly in areas like Aswan City, which has a hot and dry climate, the energy-intensive nature of these systems presents a significant issue. To address this problem, a comparative analysis of mini-split and variable refrigerant flow (VRF) systems in an Aswan city office building is being done in this study. The goal is to evaluate their energy efficiency and suitability for addressing issues related to electricity usage in this demanding environmental setting.

2. Methodology

2.1. Location and Overview of the Building

The study is carried out in a specifically chosen office building in Aswan City, Egypt, considering how it would affect sustainable energy practices. As shown in Fig. 1(a, b), The two-story facility, which has 28 offices with 270 square metres of floor area, is open from 9 a.m. to 5 p.m., consistent with the typical weekday schedule in the area and building construction shown in Table 1[9]–[12].

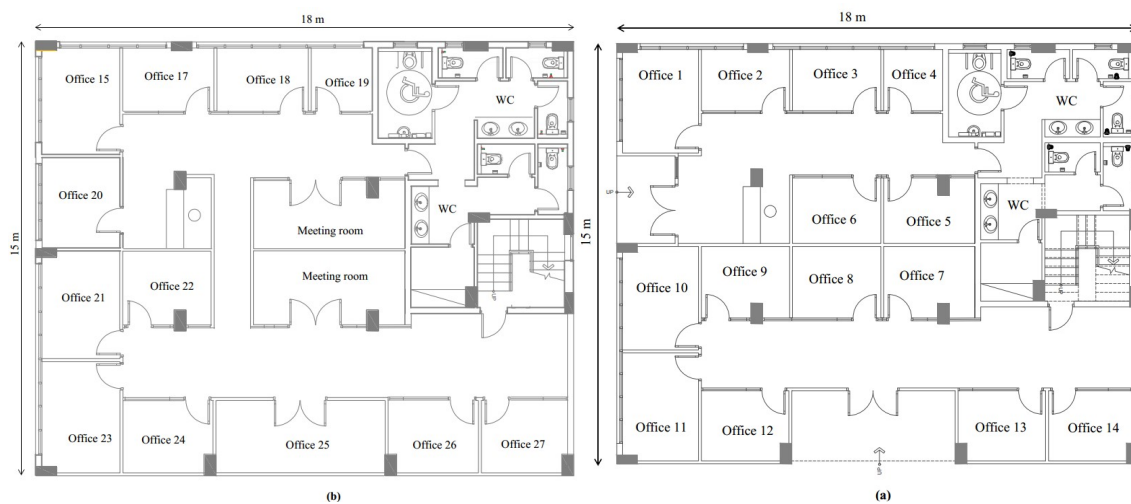


Fig. 1 Office building under investigation

2.2. Air Conditioning System Selection

The suitability of two air conditioning systems for energy efficiency and efficient ventilation is examined. These systems were chosen because they preserve indoor environmental quality and maximise energy consumption. Fans are a feature of both systems that guarantee appropriate ventilation and air movement.

2.2.1 VRF Systems, or variable refrigerant flow

The VRF system will undergo a thorough examination that includes an assessment of its energy efficiency, cooling capabilities, and suitability for the hot and dry climate that Aswan City experiences.

Table 1 The investigation's office building construction

Element	Description	U (W/m ² .K)	SC	SHGC	Area (m ²)
Roof		0.229	--	--	270
	Outside surface resistance		--	--	
	100 mm light concrete		--	--	
	125 mm insulation		--	--	
	100mm light concrete		--	--	
	20mm plaster		--	--	
	25mm stucco		--	--	
	Inside surface resistance		--	--	
Exterior Wall		2.85	--	--	--
	Outside surface resistance		--	--	--
	25mm stucco		--	--	--
	100 mm brick		--	--	--
	20mm plaster		--	--	--
	Inside surface resistance		--	--	--
North wall	--	--	--	--	58
South wall	--	--	--	--	58
East wall	--	--	--	--	99
West wall	--	--	--	--	49
Window	3mm single glazing, uncoating clear	5.55	0.64	0.78	--
North window	--	--	--	--	68
South window	--	--	--	--	68
East window	--	--	--	--	6
West window	--	--	--	--	56
Lights	12 W/m2				
People (No-activity) [12]	75-light work (75W sensible heat, 55 W latent heat)	--	--	--	--
Desktop Computer (No-Watt)	(75-144W)	--	--	--	--
Monitor (No-Watt)	(150-90W)	--	--	--	--
Printer (No-Watt)	(75-222W)			--	--
Ventilation (combined outdoor air rate) (number of people, L/s. person) [9]	(75, 8.5 L/s/person) (1.21 ACH)	--	--	--	--

2.2.2 Mini-Split System

The Mini-Split system will be thoroughly inspected, emphasising energy usage, cooling effectiveness, and adaptation to the unique requirements of the structure.

3. Modeling using TRNSYS.

Write here Using hourly weather data for the entire year, TRNSYS software (version 16) can simulate the energy used by a building's heating and cooling systems. A model is created by TRNSYS using the TRNSYS studio, which consists of components that may be found in the TRNSYS library and are connected via constant parameters, input variables, and output variables. The necessary components can be developed or bought from a third party if they are not present in the TRNSYS library. Fig. 2 displays the TRNSYS model for the current investigation. The TRNBUILD programme executes the building simulation and is connected to the TRNSYS programme via type 56 [13]. TRNBUILD is software that can simulate transient cooling and heating in a structure and heat fluxes from ventilation, lighting, humans, infiltration, and other internal and external heat sources [14]. The following is the governing equation (1) for delivering the cooling load q_{sys} , which is the transfer of heat to the cooling system (W) at each time step, and the system capacity and power consumption regression models:

$$q_{sys} = q_{conv,t} + q_{conv,IS} + q_{vent} + q_{Inf} \quad (1)$$

The variables $q_{conv,t}$, $q_{conv,IS}$, q_{vent} , and q_{inf} denote the respective contributions of convection heat transfer from all surfaces within the zone, convection heat transfer from internal heat sources, ventilation heat gain, and infiltration heat gain to the overall heat load [15], [16].

Table 2 presents the capacity and power regression models eq. (3, 4). The coefficient of performance was calculated according to equation (2). The cooling systems modulate under full load during typical operation.

$$COP = Q/p \quad (2)$$

$$P = a_0 + a_1 T_{dbi} + a_2 T_{wbi} + a_3 T_{dbo} \quad (3)$$

$$Q = b_0 + b_1 T_{dbi} + b_2 T_{wbi} + b_3 T_{dbo} \quad (4)$$

Where COP is the coefficient of performance, P is the power consumption, Q is the capacity, T_{dbi} is the indoor dry bulb temperature, T_{wbi} is the wet bulb temperature, T_{dbo} is the outdoor dry bulb temperature, a_0 to a_2 , and b_0 to b_2 are the characteristic parameters of power and capacity, respectively.

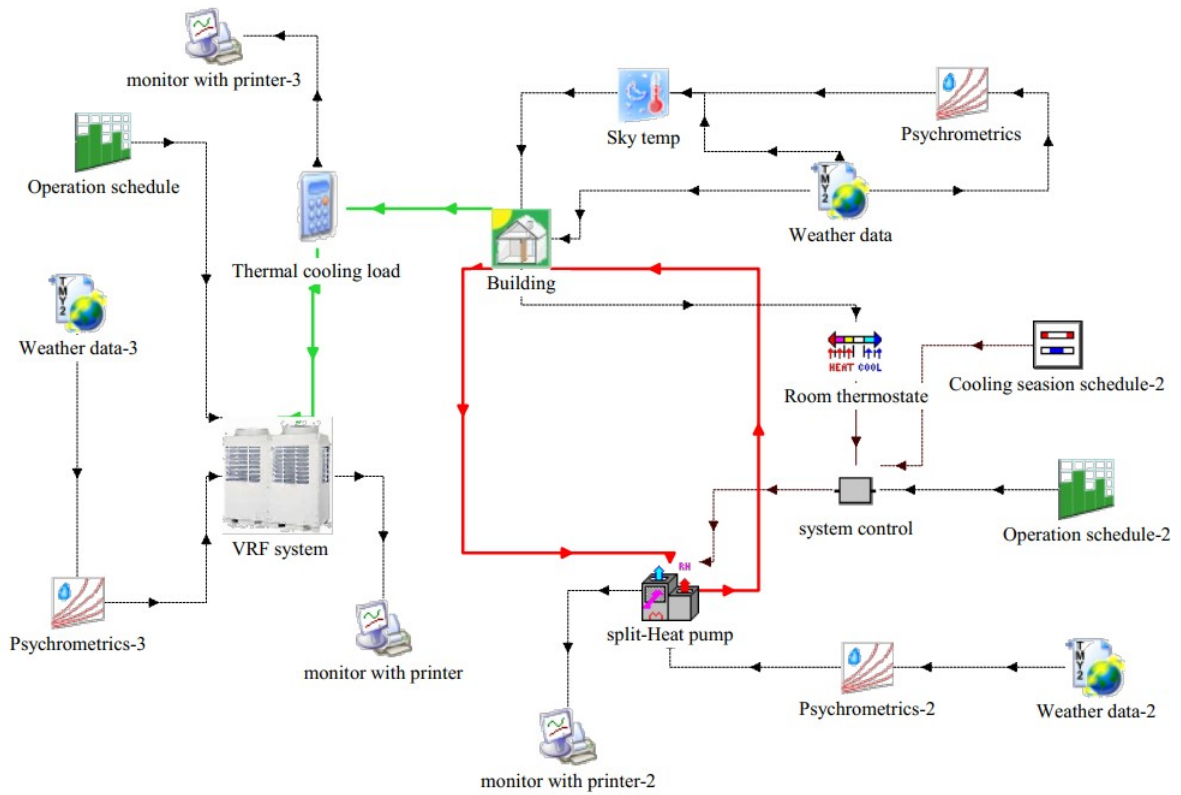


Fig. 2 TRNSYS model

3.1 Validation of the simulation model

HVAC system modelling and simulation are crucial for optimizing energy use and guaranteeing occupant comfort in buildings. Validation of simulation results against calculated results is critical for establishing the reliability and usefulness of these models. The model validation findings for weather conditions include wet and dry bulb temperatures, cooling load, as well as the energy consumption of two HVAC systems: mini-split air conditioning (MSAC), and VRF. The resulting average absolute relative error percentages serve as measures of the simulation models' fidelity and correctness. By comparing the absolute difference between the calculated value and the simulated value relative to the calculated value itself, the Average Absolute Relative Error (AARE) is a metric used to quantify the correctness of a computation or simulation. It gives an indication of the relative errors' typical magnitude.

$$ARE = \left| \frac{x_C - x_S}{x_C} \right| \tag{5}$$

The average of the absolute relative error over the number of calculations (n) is known as the average absolute relative error (AARE).

$$AARE = \frac{1}{n} \sum_{i=1}^n \left| \frac{x_{C,i} - x_{S,i}}{x_{C,i}} \right| \tag{6}$$

4. Results

4.1. Meteorological data

Figure 3 displays the Aswan City meteorological data that was extracted from a standard meteorology annual weather file from the TRNSYS library [17]. The weather at the study site is frequently hot and dry in the summer, as the figure illustrates. Throughout the year, the average outdoor temperature fluctuates between 15.3 °C and 33.6 °C, while the relative humidity ranges between 17.9% and 41%. In addition, the maximum summer temperature is 46.3 °C and the seasonal temperature is 44 °C[19]. The climate classification of Aswan City is BWh(B: arid, W: desert, and h: hot arid) desert hot-arid climate according to Koppen-Geiger and 0B according to ASHRAE, which means extremely Hot-dry climate [18], [19].

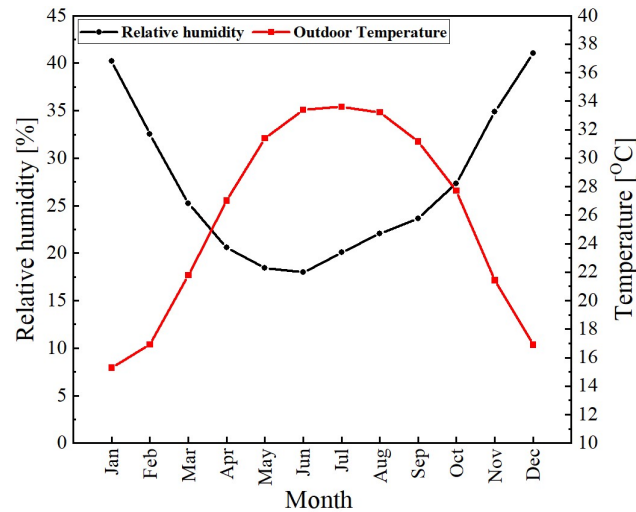


Fig. 3 The average monthly climate in Egypt's Aswan City

4.2. Building cooling load

As depicted in Fig. 4, There is a noticeable seasonal change in the cooling demand statistics for the office building in Aswan City, Egypt. The cooling load in January (ranging in hours from 0 to 744) and February (ranging in hours from 744 to 1416) throughout the winter varied from 50 kW to 75 kW, suggesting a comparatively temperate climate. The cooling load rose from 100 kW to 140 kW as the year went on and into the spring months of March through May (ranging in hours from 1416 to 3624). This increase aligns with the rising ambient temperatures, which calls for more cooling. The cooling load fluctuated most noticeably from June to October(ranging in hours from 3624 to 7296), ranging from 145 kW to 160 kW in value. In June, 161 kW was the most significant cooling load recorded. However, the cooling load dropped in November and December last year(ranging in hours from 7296 to 8760), ranging from 110 kW to 50 kW.

The cooling load peak, 161 kW in June, is an essential factor to consider. The peak load indicates when the building's cooling system is under the highest stress. It significantly affects HVAC system sizing, building design, and related energy expenses. These results emphasize the need for cooling system designs to effectively handle peak loads, guarantee passenger comfort, and lower energy usage during crucial times. The monthly cooling capacity surpasses 18 MWh in April, peaking in

July with 32.3 MWh, as shown in Fig. 5, while the required need for cooling is 189.4 MWh. From April to October.

The information emphasises how directly the hot, dry weather of Aswan City affects the cooling burden. The summer's severe temperatures and arid conditions are the leading causes of the sharp increase in cooling demand. Understanding the impact of climate change is crucial for devising suitable approaches and technologies that can effectively tackle the distinct obstacles posed by these areas.

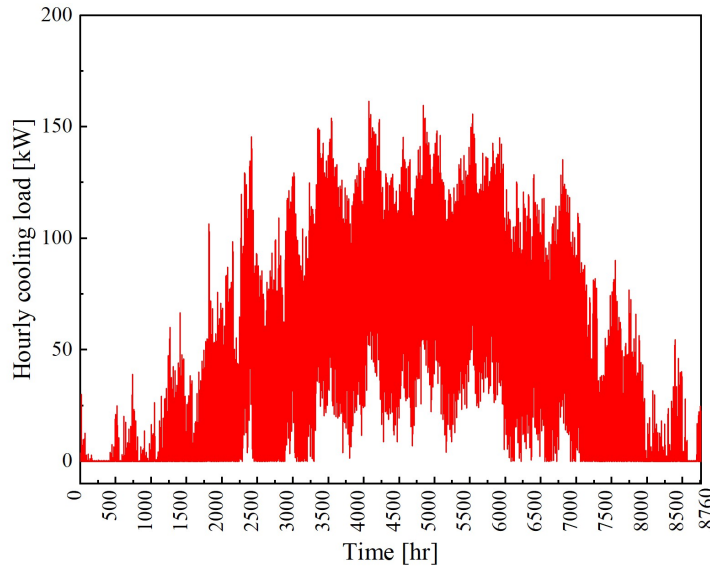


Fig. 4 Office building’s hourly cooling load throughout the year.

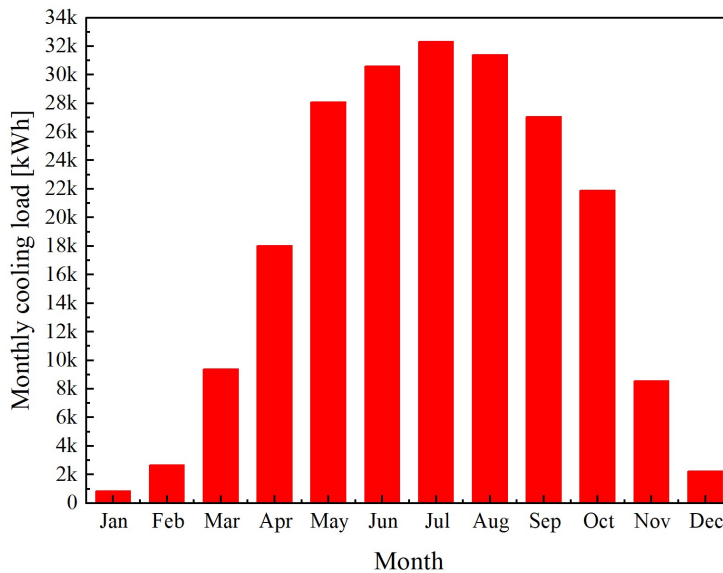


Fig. 5 Throughout the year, the examined structure's monthly cooling load

4.3. VRF system selection

Choosing a suitable inside unit is a vital first step in guaranteeing an HVAC system's peak performance and energy economy. In this case, the selection procedure is based on two primary parameters: the intended zone setpoint temperature, which might not coincide with

the nominal load conditions, and the actual maximum cooling load, as ascertained by TRNSYS simulation. Table 2 is a valuable reference that displays the regression models for capacity and power consumption of all inside units according to the catalogue [20]. These models are critical in anticipating each unit's performance characteristics under various load levels. HVAC engineers and designers can make educated selections by including these regression models in the selection process, matching the system's capacity and power consumption with the specific requirements of the zone or space. Additionally, the setpoint indoor dry bulb and wet bulb temperatures are 25°C and 18°C ,respectively, for the thermal comfort of the occupants. This method improves energy efficiency and ensures occupant comfort while remaining energy-efficient and environmentally responsible.

4.4. MSAC system selection

A critical component that increases the system's capacity and guarantees a suitable interior climate is its operational flexibility, which allows it to change its pace in response to changing cooling demands. To demonstrate the regression models for the capacity and power consumption of the chosen units inside the building according to manufacturing data [20], Table 2 is essential. These models were created to emphasise the cooling load connected to every individual zone. In addition, for the inhabitants' thermal comfort, the setpoint interior dry bulb and wet bulb temperatures are 25 °C and 18 °C, respectively.

Table 2 Regression model of VRF and Mini-split Systems.

Type	Capacity	Regression model	No of unit	R-sq (%)
MSAC	24,000 Btu/hr.	$Q = -1.014 - 0.01648 T_{odb} + 0.345 T_{idb} - 0.082 T_{iwb} \text{ (kW)}$	20	92.66
		$P = -1.500 + 0.03721 T_{odb} + 0.1717 T_{idb} - 0.1418 T_{iwb} \text{ (kW)}$		94.85
VRF	140 kW	$Q = -14.63 - 0.6769 T_{odb} + 8.29 T_{idb} - 2.89 T_{iwb} \text{ (kW)}$	1	88.41
		$P = -25.53 + 0.4831 T_{odb} + 2.802 T_{idb} - 2.150 T_{iwb} \text{ (kW)}$		94.14

4.5. Validation of system modeling

Figure 2: A schematic representation of the TRNSYS model displays the TRNSYS model for each of the two HVAC systems that are recommended. Due to the start of the working year and the crowded facility with staff members, the model validation was completed on July 3. Using the weather data from the TRNSYS library and cross-checking it with meteorological data obtained from the ENER-WIN programme, which is reliant on the World Meteorological Organisation (WMO) and ASHRAE standard 90.1-2016[13], [17]. Ener-Win, developed originally at Texas A&M University, models hourly energy usage in buildings, including annual and monthly energy consumption, peak demand charges, peak heating and cooling loads, solar heating percentage through windows, daylighting contribution, and a life-cycle cost analysis. The design data is summarised per zone and includes duct sizes and electrical power needs. Ener-Win software is made up of multiple

components, including an interface module, a meteorological data retrieval module, a sketching module, and an energy simulation module. The interface module contains a basic construction sketching interface. Ener-Win takes only three fundamental inputs: (1) the building type, (2) the location of the building, and (3) the geometrical data of the building[21]. The variations between the wet and dry bulb temperature values are shown in Fig. 5. Using Table 5-Table 11 For cooling load validation in this study, the Cooling Load Temperature Difference (CLTD) method is used according to ASHRAE Fundamentals [9]–[11], [22]. The comparison of the calculated and simulated values of cooling load is shown in Fig. 7. The comparison of the calculated and simulated energy consumption of two HVAC systems is shown in Fig. 8(a, b). The figures show an appropriate match with the calculated and simulated values. For both Outdoor Wet Bulb (OWB) and Outdoor Dry Bulb (ODB) temperatures, respectively, the AARE values for the weather are 0.9% and 12.9%, respectively. According to the validation analysis, the average absolute relative error of the cooling load was 4.56% between the CLTD method and TRNSYS. The average absolute relative error for an MSAC system was 4.56%, while for a VRF system, it was 4.28%. In addition, the MSAC system had ARE ranging from 8.7% to 0.04%, while the VRF system had ARE ranging from 7.6% to 0.74%. These validation findings show that the simulation models for two HVAC systems are highly accurate and reliable. The small differences between the simulation and calculated findings support the appropriateness of these models for precise system behaviour and performance predictions. The results of this investigation offer a substantial contribution to the field of energy-efficient building design and operation. To make well-informed judgements, optimise energy consumption, and ensure occupant comfort, engineers and practitioners can reliably rely on these simulation models.

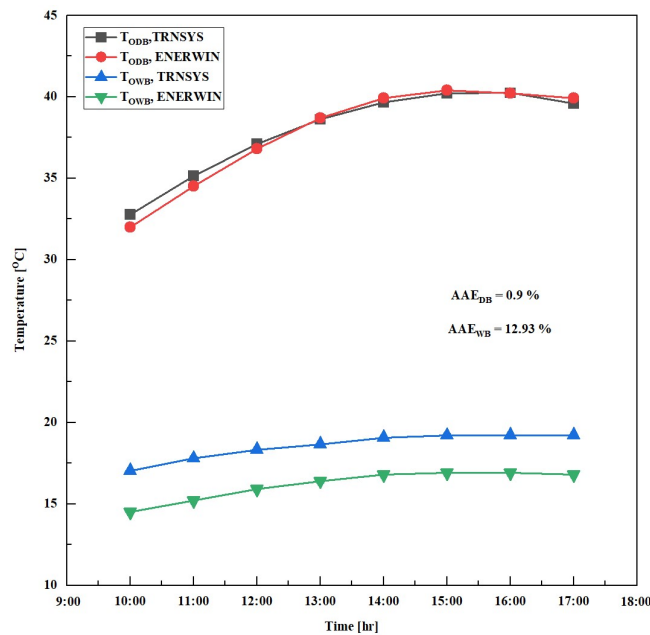


Fig. 6 Comparison of TRNSYS and ENER-WIN dry bulb and wet bulb temperature values for meteorological conditions for Aswan city.

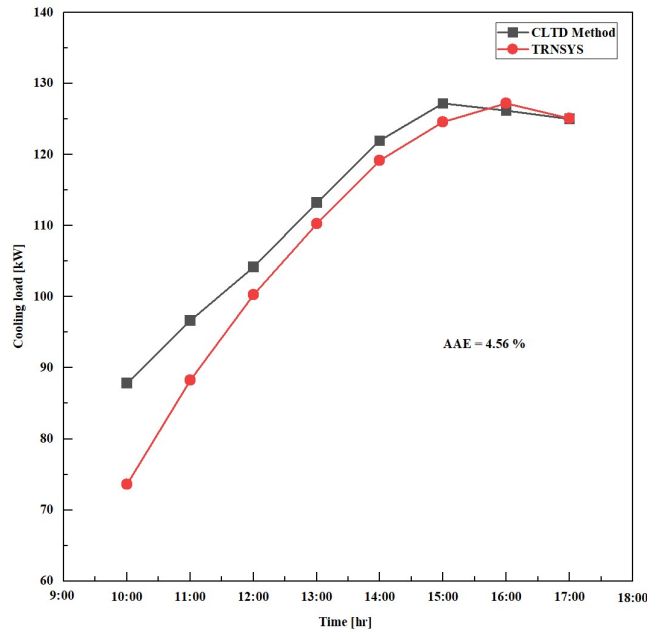


Fig. 7 Comparison of CLTD method and TRNSYS for cooling load.

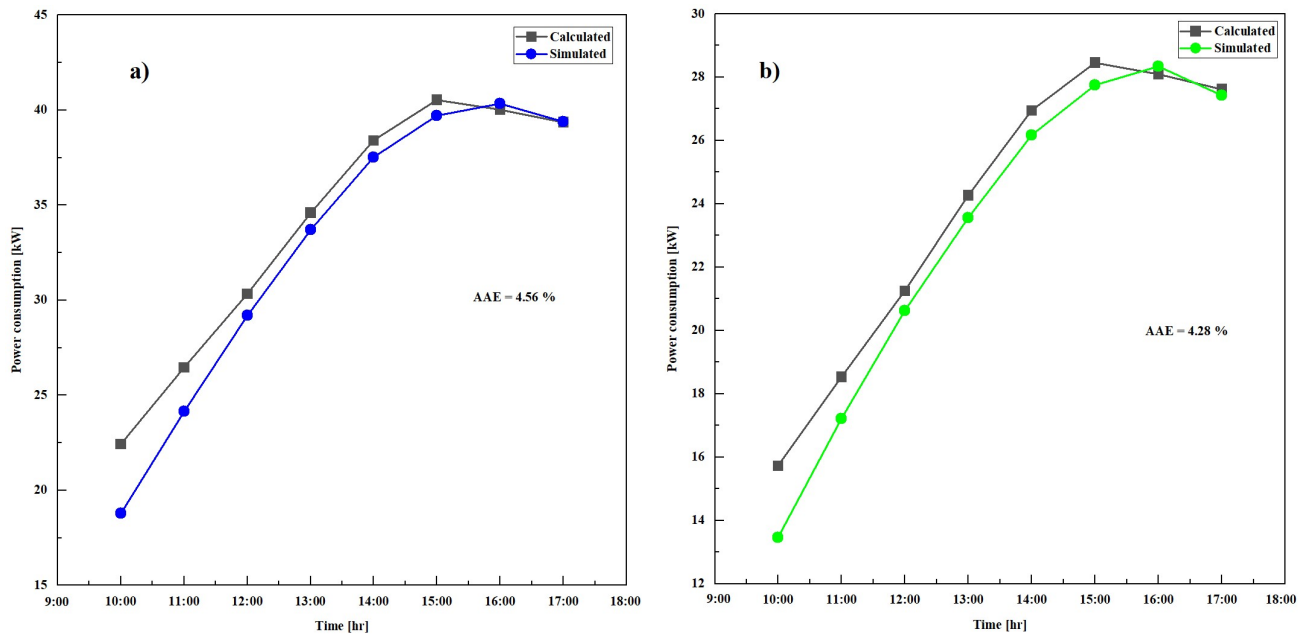


Fig. 8 A comparison of the calculated and simulated energy consumption values for two HVAC systems. (a) MSAC system. (b) VRF system.

4.6. Performance of the MSAC system and the VRF system

This study thoroughly compared the energy performance of two different HVAC systems: the Mini-Split Air Conditioning (MSAC) system and the Variable Refrigerant Flow (VRF) system. Over a year, the data, reported in kilowatts per hour (kWh), yielded numerous significant observations. When compared to the MSAC system, the VRF system continuously showed reduced energy consumption throughout the year, as shown in Fig. 9. Significantly, the VRF system continued to have a significant energy efficiency advantage

in the hot summer months of June, July, and August, using about 6243.75 kWh in June and 6476.95 kWh in July, as opposed to the MSAC system's higher consumption of about 8494.14 kWh and 8815.92 kWh, respectively. These results reaffirm the VRF system's well-known ability to operate energy-efficiently.

Moreover, a more detailed data analysis revealed seasonality in both systems' energy usage patterns. With an estimated 3167.59 kWh consumed in December, the MSAC system's energy usage increased during the colder months, indicating that it would be less effective at preserving indoor comfort during inclement weather. Conversely, the VRF system's energy usage varied from 1642.38 kWh in January to 6409.76 kWh in August, demonstrating a more balanced energy performance throughout the seasons and its resilience to changing climatic circumstances.

In addition, In the context of energy-efficient technologies and design strategies for HVAC systems, it is crucial to examine the energy consumption of specific systems under various operational loads. A comparative analysis was conducted on the energy consumption of two prominent HVAC systems, the Mini-Split Air Conditioning (MSAC) system and the Variable Refrigerant Flow (VRF) system, at different loads—100%, 75%, and 50% as illustrated in Fig.10.

At 100% load, the MSAC system exhibited an energy consumption of 57.46 MWh, which decreased to 35.16 MWh and 23.44 MWh at 75% and 50% loads, respectively. In contrast, the VRF system demonstrated superior energy efficiency, with consumption figures of 42.5 MWh, 24.68 MWh, and 16.45 MWh at 100%, 75%, and 50% loads, respectively.

Additionally, evaluating the systems based on the average coefficient of performance (COP) throughout their operation further underscores the efficiency contrast. The VRF system had an average COP of 5.5, 4.3, and 3.8 compared with 3.8, 3.2, and 2.5 for the MSAC system under 100%, 75%, and 50% load conditions, respectively.

This data substantiates the conclusion that, despite achieving the desired thermal comfort in indoor spaces, the VRF system consistently consumes less energy across various operational loads. As such, embracing energy-efficient technologies such as the VRF system, coupled with thoughtful design strategies, emerges as a key approach to not only reduce environmental impact but also optimise long-term energy costs in HVAC applications which are discussed in the following section 4.8 and 4.9.

With the hot, dry summer mode operation applied to Aswan, Figure 11 shows the cooling process on the psychrometric chart. The incoming state of the cooling coil in this mode is called mixed air condition "m," which is created by combining outside air at state "o" with room air that has been circulated (stat "R"). Following that, the air is cooled and made less humid until it leaves the coil in state "cc." After that, the heat gain from the electric motor of indoor units' fans, causing the supply condition to state "s." Here are the expressions for the latent, sensible, and total loads in space, as follows:

$$Q_{R,S} = m_s (h_r - h_s) \tag{7}$$

$$Q_{R,L} = m_s (h_r - h_r') \tag{8}$$

$$Q_{R,T} = m_s (h_r - h_s) \tag{9}$$

Where, Q denotes the load quantity and the enthalpies contain subscripts that correspond to the points identified on the psychrometric chart. The supply mass flow rate can be calculated using either of these equations. The supply volume flow rate, on the other hand, is calculated using the specific volume at the supply condition. This is stated as follows:

$$\mathcal{V}'_s = m_s \mathcal{V}_s \quad (10)$$

On the psychrometric chart, line "S R" represents the space (room) sensible heat ratio (RSHR). The following equations apply to cooling load coil (or grand) loads:

$$Q_{G,s} = m_s (h_m - h_{cc}) \quad (11)$$

$$Q_{G,L} = m_s (h_{m'} - h_m) \quad (12)$$

$$Q_{G,T} = m_s (h_m - h_{cc}) \quad (13)$$

Once again, the subscripts of the enthalpy quantities correlate to state points on the chart. The formulae can be used to calculate the size of the cooling coil. The grand (or cooling coil) sensible heat ratio (GSHR) is shown graphically by the line "m cc". The latent, sensible, and total loads are 7 kW, 138 kW, and 145 kW, respectively.

According to ASHRAE climate design conditions [11], [23], with an annual dry-bulb temperature of 44°C and a wet-bulb temperature of 22°C, this study meticulously examines the intricate interplay between cooling load and variable refrigerant flow (VRF) system capacity. The simulation data, spanning May, July, and September, reveals cooling loads of 121 kW, 114 kW, and 139 kW, respectively, juxtaposed against corresponding VRF system capacities of 125 kW, 127 kW, and 140 kW, which correspond to the annual dry-bulb temperature from the ASHRAE station as mentioned previously. Notably, the cooling loads closely align with or slightly fall below the VRF system's capacities in each instance, underscoring the system's robustness in effectively managing and meeting the cooling demands. This alignment ensures the system operates within its optimal range even under challenging climatic conditions. Leveraging ASHRAE station data for dry-bulb and wet-bulb temperatures, this study adeptly navigates the nuanced challenges associated with elevated ambient temperatures. Importantly, it is highlighted that the VRF system, despite the demanding conditions, consistently achieves thermal comfort by efficiently handling the cooling loads, ensuring occupants experience optimal indoor temperatures throughout the evaluation period.

These results highlight the possible energy efficiency advantages of using the VRF system instead of the MSAC system, especially in areas with varying climates. The study's findings not only further the conversation on environmentally friendly HVAC systems but also provide building managers and legislators with helpful information for maximising energy efficiency and minimising adverse environmental effects. This study is a valuable tool for individuals seeking to pick HVAC systems to achieve sustainability and energy efficiency.

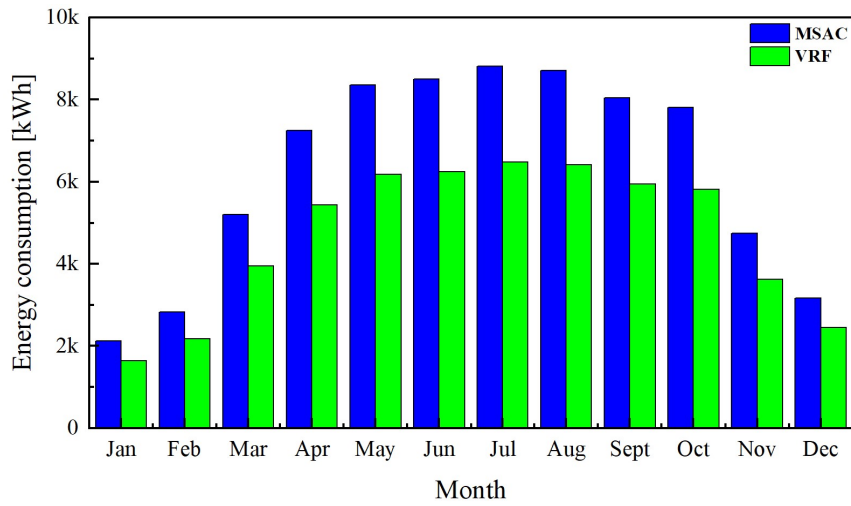


Fig. 9 Monthly energy consumption for VRF system and MSAV system

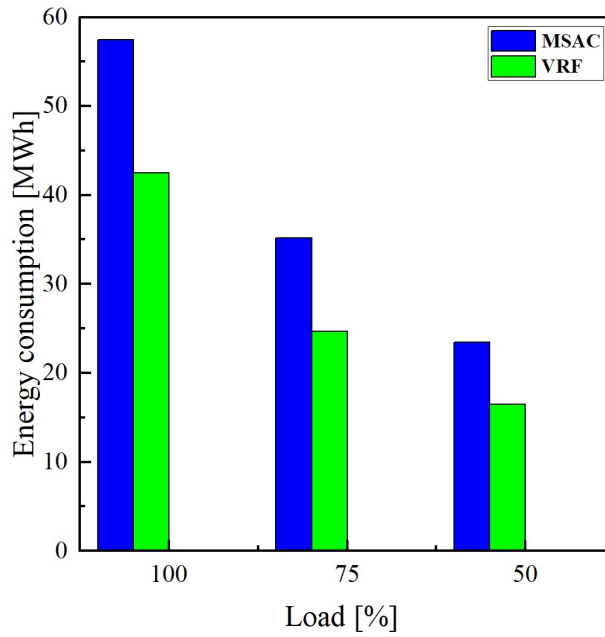


Fig. 10 Energy consumption at different loads for two HVAC systems (MSAC and VRF)

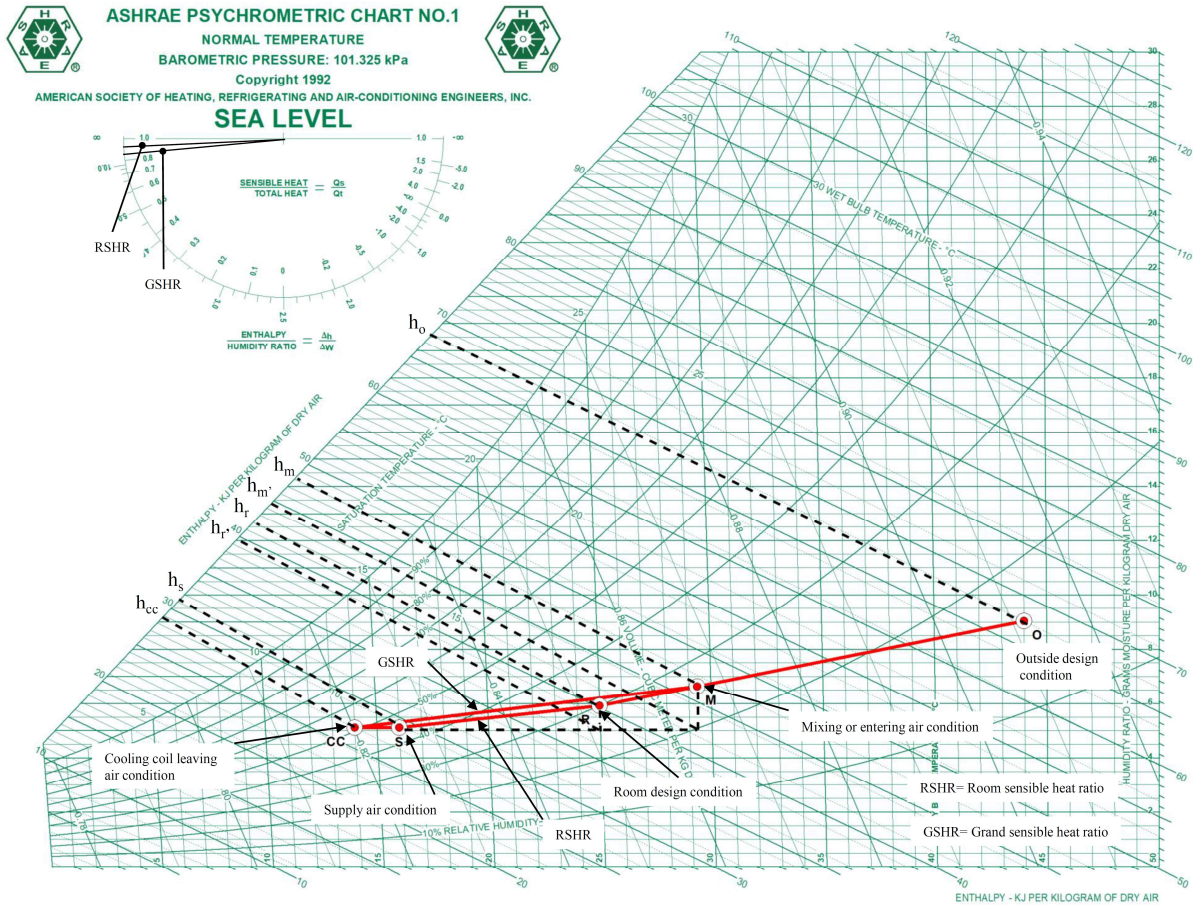


Fig. 11 Schematic for cooling process on psychrometric chart.

4.7. Energy saving

With an emphasis on evaluating their energy efficiency and possible energy savings, Fig. 12 shows the yearly energy consumption of two well-known HVAC systems, the Multi-Split Air Ventilation (MSAC) and Variable Refrigerant Flow (VRF) systems. The information, which is presented in kilowatt-hours (kWh), offers a thorough picture of their annual energy usage; the MSAC system registered a substantially more significant amount of energy at roughly 75,519.36 kWh, while the VRF system consumed roughly 56,331.93 kWh. According to the data, the VRF system uses significantly less energy annually than the MSAC system. This difference in energy use demonstrates the VRF system's better energy efficiency. We can compute the ratio of the VRF's energy consumption to the MSAC system's energy consumption to determine energy efficiency. With this ratio of roughly 0.746, it can be inferred that the VRF system uses roughly 74.6% of the energy used by the MSAV system. These numbers confirm the VRF system's well-known energy-efficient performance.

Switching to the VRF system can result in significant energy savings, as seen by the notable difference in annual energy consumption between the two systems. We may calculate these possible savings by deducting the VRF system's yearly energy use from the MSAC system,

which comes out to be about 19,187.43 kWh. This is an estimate of the possible energy savings that the VRF system can provide. A move like this might save energy usage, result in significant financial savings, and more crucially, help reduce greenhouse gas emissions, which would boost environmental initiatives.

The study's conclusions have essential ramifications for stakeholders concerned about energy use, including building managers and policymakers. The data demonstrates the improved energy efficiency of the VRF system and emphasises the advantages of implementing it in building HVAC systems. A change of this kind might result in yearly energy savings of about 19,187.43 kWh, which illustrates the practical implications. This research offers priceless insights for decision-makers looking to optimise energy use and improve energy sustainability in various environmental scenarios. The study's conclusions add to the conversation about sustainable HVAC solutions and, consequently, the larger objectives of lowering energy use and lessening environmental effects. These objectives are essential to the global effort to develop sustainable and energy-efficient construction techniques.

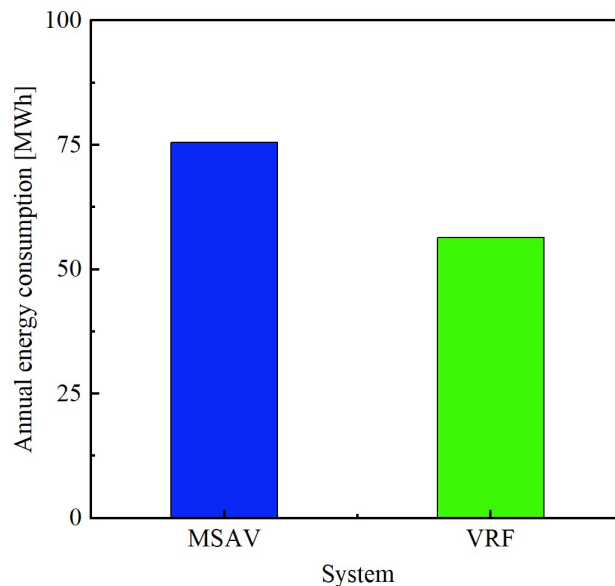


Fig. 12 Annual Energy consumption of the VRF system and MSAV system

4.8. Cost Analysis

One useful metric for determining if energy efficiency initiatives are financially feasible is the payback period. The time it takes for energy savings from a more efficient system to offset the initial installation costs is referred to as the payback period in the context of HVAC systems. The building under consideration has a 40-tonne refrigeration total cooling requirement, and the average price of electricity globally is 0.192 USD per kWh [24]. For the MSAC and VRF systems, respectively, initial and installation costs per ton of refrigeration are 942 USD, 2081 USD and total maintenance costs are 1572.4 USD and 634.9 USD for the MSAC and VRF systems, respectively according to local prices. Table 1 assesses each system's total energy usage for the study's operational time, which ran from April to October, based on the simulation's results. The VRF system has a payback period of 8.29 years.

Table 3 The VRF system payback period

Item	VRF	MSAC
Total initial and installation costs [USD]	81,178.5	37,680
Total running cost [USD]	12,876.6	18,120.8
Difference in running cost [USD]	5,244.26	
Difference in initial and installation costs [USD]	43,498.5	
Payback period	8.29	

4.9. Environmental impact

The estimated prevented CO₂ emissions in this study are calculated using a three-fuel emission factor. The CO₂ emissions for the two cooling systems on an annual basis have been determined. This has been achieved by utilizing an emission factor that is multiplied by the annual energy consumption. The purpose of this research was to compare the CO₂ emissions produced by two different air conditioning systems that were fuelled by coal, oil, and natural gas. At this point, the amount of carbon dioxide (CO₂) emission from coal, oil, and natural gas is calculated. Table 4 illustrates the CO₂ released in kg/kWh, and the average is taken [25], [26]. The results of this study show that, among all fuel types, the VRF system had the lowest CO₂ emissions. As seen in Fig. 13, the VRF system emitted 41.4, 32.9, and 23.4 metric tons less CO₂ when fuelled by coal, oil, and natural gas, respectively, than the MSAC system (which emitted 56, 44.5, and 31.6 metric tonnes). The VRF system saves about 26.03% of greenhouse emissions, so the VRF system is considered environmentally friendly. These results indicate that using a VRF system can significantly reduce air conditioning systems' carbon footprint, hence contributing to environmental sustainability.

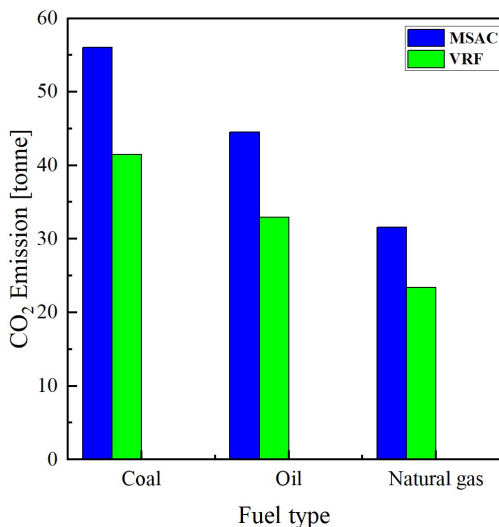


Fig. 13 Annual CO₂ emissions for the two cooling systems (Mini-split AC, and VRF system) based on the fuel type (coal, oil, and natural gas)

Table 4 CO₂ emissions factor in kilograms for every kWh of electricity generated [26].

Fuel	Coal	Petroleum oil	Natural gas
CO ₂ emitted in kg/kWh	0.95 to around 1	0.75 to around 0.8	0.55

5. Conclusion

An urgent problem in Egypt is the high electricity consumption levels brought on by the widespread use of air conditioning equipment in buildings. Particularly in areas like Aswan City, which has a hot and dry climate, the energy-intensive nature of these systems presents a significant issue. To address this problem, a comparative analysis of mini-split air-conditioning (MSAC) and variable refrigerant flow (VRF) systems in an Aswan city office building is being done in this study using TRNSYS software. The goal is to evaluate their energy efficiency and suitability for addressing issues related to electricity usage in this demanding environmental setting.

- The VRF system continuously showed less energy use than the MSAC system, especially in the hottest summer months.
- While the MSAC system displayed higher consumption during the winter, the VRF system demonstrated balanced energy performance throughout the year.
- Switching to the VRF system might achieve significant yearly energy savings of roughly 19,187.43 kWh.
- These results offer insightful information to help decision-makers choose energy-efficient HVAC systems that support environmentally friendly building practices.
- For the MSAC system, the estimated energy efficiency ratio of the VRF system is roughly 0.746, meaning that it uses roughly 74.6% of the energy that the MSAC system uses. As a result, the VRF system uses substantially less energy for the same or comparable HVAC performance, making it roughly 74.6% more energy-efficient than the MSAC system.
- The VRF system outperformed the MSAC system, with payback periods of 8.29 years.
- The VRF system emitted 41.4, 32.9, and 23.4 metric tonnes less CO₂ when fuelled by coal, oil, and natural gas, respectively than the MSAC system (which emitted 56, 44.5, and 31.6 metric tonnes). The VRF system saves about 26.03% of greenhouse emissions.

These findings demonstrate the potential benefits of switching from the MSAC system to the VRF system regarding energy efficiency, particularly in regions with different climates. The study's conclusions not only further the discussion on eco-friendly HVAC systems but also give lawmakers and building managers practical knowledge for boosting energy efficiency and reducing adverse environmental effects. This study is a helpful resource for people choosing HVAC systems that will achieve sustainability and energy efficiency.

References

- [1] United Nations. Conference of the Parties: Twenty-First Session. United Nations - Framew. Conv. Clim. Chang., vol. 01192, no. November, p. 32, 2015, [Online]. Available: <https://unfccc.int/process-and-meetings/conferences/past-conferences/paris-climate-change->

- conference-november-2015/cop-21.
- [2] M. Caponigro, A. Manoloudis, and A. M. Papadopoulos. Developing a strategy for energy efficiency in the Egyptian building sector. *IOP Conf. Ser. Earth Environ. Sci.*, vol. 410, no. 1, 2020, doi: 10.1088/1755-1315/410/1/012076.
- [3] Climate Resilience for Energy Transition in Egypt – Analysis - IEA. <https://www.iea.org/reports/climate-resilience-for-energy-transition-in-egypt%0AAccessed:2023-10-22%0AReferenceSuccess%0A> (accessed Oct. 22, 2023).
- [4] M. A. F. Abdollah, R. Scoccia, G. Filippini, and M. Motta. Cooling energy use reduction in residential buildings in egypt accounting for global warming effects. *Climate*, vol. 9, no. 3, 2021, doi: 10.3390/cli9030045.
- [5] L. E. Singer and D. Peterson. *International energy outlook 2010*, vol. 0484, no. May. 2011.
- [6] M. Y. Arafat, A. A. Faggal, L. Khodeir, and T. Refaat. Customizing the green pyramid rating system for assessing university buildings’ sustainability: A stakeholder-involved weighting approach. *Alexandria Eng. J.*, vol. 82, no. March, pp. 446–458, 2023, doi: 10.1016/j.aej.2023.10.013.
- [7] M. Fahmy, I. Elwy, and S. Mahmoud. Back from parcel planning to future heritage of urban courtyard: The 5th generation of Egyptian cities as a sustainable design manifesto for neo-arid neighbourhoods. *Sustain. Cities Soc.*, vol. 87, no. August, 2022, doi: 10.1016/j.scs.2022.104155.
- [8] O. M. Galal, H. Mahmoud, and D. Sailor. Impact of evolving building morphology on microclimate in a hot arid climate. *Sustain. Cities Soc.*, vol. 54, no. November 2019, 2020, doi: 10.1016/j.scs.2019.102011.
- [9] J. A. B. Wissing, M. P. Wissing, M. M. du Toit, and Q. M. Temane. Ventilation for Acceptable Indoor Air Quality. ANSI/ASHRAE Standard 62.1-2010. *J. Psychol. Africa*, vol. 18, no. 4, pp. 511–520, 2008, doi: 10.1080/14330237.2008.10820230.
- [10] C. L. Principles. *Nonresidential Cooling and Heating. 1997 ASHRAE Fundam. Handb.*, 1997.
- [11] ASHRAE. *2021 Ashrae Handbook*. 2021.
- [12] ASHRAE. *Fundamentals Handbook (SI) Overloading or Underloading Nonresidential Cooling and Heating Load Calculation Procedures 2001 ASHRAE. Ashrae Stand.*, no. 1984, pp. 8–13, 2001.
- [13] S. A. Klein, W. A. Beckman, and J. A. Duffie. Trnysys - a Transient Simulation Program.. *ASHRAE Trans.*, vol. 82, no. pt 1, pp. 623–633, 1976.
- [14] M. E. Zayed, M. M. Aboelmaaref, and M. Chazy. Design of solar air conditioning system integrated with photovoltaic panels and thermoelectric coolers: Experimental analysis and machine learning modeling by random vector functional link coupled with white whale optimization. *Therm. Sci. Eng. Prog.*, vol. 44, no. March, p. 102051, 2023, doi: 10.1016/j.tsep.2023.102051.
- [15] R. L. Shrivastava, V. Kumar, and S. P. Untawale. Modeling and simulation of solar water heater: A TRNSYS perspective. *Renew. Sustain. Energy Rev.*, vol. 67, pp. 126–13, 2017, doi: 10.1016/j.rser.2016.09.005.
- [16] A. C. Megri, N. C. A. A. C. Megri, and N. C. A. TRNSYS as an Education Tool to Predict Indoor Environment Temperature for Undergraduate Students AC 2014 - 10696 : TRNSYS as an Education Tool to Predict Indoor Environment Temperature for Undergraduate Students Megri holds a PhD degree from INSA at Lyon. 2011.
- [17] Solar Energy Laboratory. TRNSYS 16: Weather Data. *Sol. Energy Lab.*, vol. 9, 2006.
- [18] M. Kottek, J. Grieser, C. Beck, B. Rudolf, and F. Rubel. World map of the Köppen-Geiger

- climate classification updated. Meteorol. Zeitschrift, vol. 15, no. 3, pp. 259–263, 2006, doi: 10.1127/0941-2948/2006/0130.
- [19] A. Addendum and A. Standard. Climatic data for building design standards. ASHRAE Stand., vol. 8400, no. 169, pp. 404–636, 2013.
- [20] H. P.. Heat Pump catalogue R410A(50Hz/60Hz). p. 326, 2015.
- [21] Ener-Win Energy Simulation Software for Buildings with Life-Cycle Costs. <http://pages.suddenlink.net/enerwin/> (accessed Dec. 16, 2023).
- [22] ASHRAE. ASHRAE handbook: heating, ventilating, and air-conditioning systems and equipment. 2020.
- [23] ASHRAE climatic design conditions. <http://ashrae-meteo.info/v2.0/index.php?lat=23.964&lng=32.820&place=%27%27&wmo=624140> (accessed Dec. 20, 2023).
- [24] Electricity prices around the world | GlobalPetrolPrices.com. https://www.globalpetrolprices.com/electricity_prices/ (accessed Dec. 07, 2023).
- [25] L. Abdallah and T. El-Shennawy. Evaluation of CO₂ emission from Egypt's future power plants. Euro-Mediterranean J. Environ. Integr., vol. 5, no. 3, pp. 1–8, 2020, doi: 10.1007/s41207-020-00184-w.
- [26] International Energy Agency (IEA). Energy, Climate Change and Environment 2016 Insights – Analysis - IEA. IEA publications, Paris, 2016. <https://www.iea.org/reports/energy-climate-change-and-environment-2016-insights> (accessed May 04, 2023).

Appendix

Table 5 Sensible heat Cooling Load Factors (CLF) for people

Total hours in space	Hours after each entry into space								
	1	2	3	4	5	6	7	8	9
8	0.51	0.61	0.67	0.72	0.76	0.8	0.82	0.84	0.38

Table 6 Cooling Load Factors (CLF) when lights are on for 8 hours.

“b” class (C)	Number of hours after lights are turned on								
“a” coefficient (0.55)	9	10	11	12	13	14	15	16	17
	0.28	0.26	0.25	0.23	0.22	0.2	0.19	0.18	0.17

Table 7 Cooling Load Temperature Differences (CLTD) for calculating cooling load from a sunlit wall.

Wall facing	Time (hr.)								
	9	10	11	12	13	14	15	16	17
North	3	3	4	5	6	7	8	10	10
South	2	3	5	7	10	14	16	18	19
East	10	15	18	20	21	21	20	19	18
West	3	4	4	5	6	8	11	15	20

Table 8 Cooling Load Factors (CLF) for glass with interior shading, north latitudes.

Wall facing	Time (hr.)								
	9	10	11	12	13	14	15	16	17
North	0.73	0.8	0.86	0.89	0.89	0.86	0.82	0.75	0.78
East	0.76	0.62	0.41	0.27	0.24	0.22	0.2	0.17	0.14
West	0.13	0.15	0.16	0.17	0.31	0.53	0.72	0.82	0.81
South	0.38	0.58	0.75	0.83	0.8	0.68	0.5	0.35	0.27

Table 9 Maximum Solar Heating Gain Factor (SHGF), W/m² for sunlit glass, north latitudes (24°)

Month	North	South	East	West
July	142	145	672	672

Table 10 Cooling Load Temperature Differences (CLTD) for calculating cooling load from flat roofs.

CLTD	Hours after each entry into space								
	9	10	11	12	13	14	15	16	17
		9	8	8	8	9	11	14	16

Table 11 CLTD correction for Latitude and Month (LM) applied to Walls and Roof, north latitude (24°)

Month	North	South	East	West	Horizontal
July	0.5	-3.3	0	0	0.5